Supporting Information for "The influence of tidal heating on the Earth's thermal evolution along the dynamical history of the Earth-Moon system"

S. H. Luna[1], M. G. Spagnuolo[2], H. D. Navone[3,4]

[1]Instituto de Estudios Andinos "Don Pablo Groeber" (IDEAN). Universidad de Buenos Aires – CONICET. Intendente Güiraldes 2160,

Ciudad Universitaria, Pabellón II, C1428EGA, Ciudad Autónoma de Buenos Aires, Argentina.

[2]Instituto de Estudios Andinos "Don Pablo Groeber" (IDEAN). Universidad de Buenos Aires – CONICET. Intendente Güiraldes 2160,

Ciudad Universitaria, Pabellón II, C1428EGA, Ciudad Autónoma de Buenos Aires, Argentina. E-mail: mgspag@gmail.com

[3]Facultad de Ciencias Exactas, Ingeniería y Agrimensura. Universidad Nacional de Rosario. Av. Pellegrini 250, S2000BTP, Rosario,

Argentina.

[4]Instituto de Física de Rosario (IFIR). CONICET – Universidad Nacional de Rosario. Bv. 27 de Febrero, S2000EKF, Rosario,

Argentina.

Contents of this file

Introduction

May 27, 2021, 10:50am

In this document we present the derivation of the general expression for the heat flux through a conductive lid in a setting where heat transport is dominated by convection, together with the corresponding figures. In addition, we reproduce the expression of $H(t)$, i.e. the rate at which heat is produced by decay of radioactive elements, and the functional form of the quality factors $K_{\mathrm{I}}(l, \chi_{lmpq})$ present in the expression of the tidal heating rate. Tables S1, necessary for the computation of $H(t)$, Tables S2 and S3 are also included for the implementation of the numerical models.

Text S1. Derivation of the convecting heat flux expressions

The dominant heat transfer mechanism inside Earth is convection on geological time scales. In our work, we will make use of the *boundary layer approach* (Turcotte & Schubert, 2014) in order to obtain simple expressions of the heat flow in the convection regime. Briefly speaking, under specific circumstances, the temperature profile of a fluid in the thermal convection regime, flowing over or below a heated or cooled surface, can described as a temperature profile corresponding to thermal conduction through a thin lid followed by an isothermal profile (see Figure S2).

The Nusselt number is defined as the ratio of heat flux transported by convection to that by conduction (Turcotte & Schubert, 2014). Mathematically expressed:

$$\mathrm{Nu} = \frac{q^{\mathrm{conv}}}{q^{\mathrm{cond}}} \tag{S-1}$$

By virtue of what we have pointed out before, we then have that $\mathrm{Nu} \gg 1$. Another useful definition of the Nusselt number, that fits the purposes of our work, is the following (Turcotte & Schubert, 2014):

$$\mathrm{Nu} = \left(2^4 \frac{\mathrm{Ra}}{\mathrm{Ra_{cr}}}\right)^{\frac{1}{3}}, \tag{S-2}$$

where Ra is the Rayleigh number and $\mathrm{Ra_{cr}}$ is the critical value of the Rayleigh number (Turcotte & Schubert, 2014). The Rayleigh number is defined as:

$$\mathrm{Ra} = \frac{\alpha \, \rho \, g \, \Delta T \, d^3}{\kappa \, \eta}, \tag{S-3}$$

where α is the thermal expansivity coefficient, g is the surface gravitational acceleration, ΔT is the temperature difference between the limiting surface and the limit of the conduction lid of thickness d, closest to the former. In addition, $\kappa = k \, (c \, \rho)^{-1}$ is the thermal diffusivity and η is the dynamical viscosity.

Equating Equations (S-1) and (S-2) leads to:

$$q^{\mathrm{conv}} = \left(2^4 \frac{\mathrm{Ra}}{\mathrm{Ra_{cr}}}\right)^{\frac{1}{3}} q^{\mathrm{cond}}. \tag{S-4}$$

In order to derive the expression of the conductive thermal flux, consider the volume enclosed by two concentric spherical surfaces, which we assume it is filled with a solid material. The inner spherical surface has radius R_{in} and it is at temperature T_{in}, while the outer one has radius R_{out} and it is at temperature T_{out} (see Figure S1) which is assumed to be less than T_{in} ($T_{\mathrm{out}} < T_{\mathrm{in}}$).

If we assume that heat transfers within the material enclosed by the concentric spherical surfaces by conduction, then the temperature profile inside the volume can be found by virtue of the Fourier's law:

$$\mathbf{q} = - \, k \, \nabla T \tag{S-5}$$

where k is the thermal conductivity of the material and T is the temperature. In the following, some simplifying assumption will be considered. First, we will consider the temperature distribution in the steady state. In consequence, the time derivative of the

energy density is equal to zero and the equation expressing the energy conservation law:

$$\frac{\partial u}{\partial t} + \nabla \cdot \mathbf{q} = \varrho \left(\mathbf{r}, t \right), \tag{S-6}$$

becomes:

$$\nabla \cdot \mathbf{q} = 0. \tag{S-7}$$

In addition, we will assume that heat flows radially outwards the hollow sphere. This implies that $\mathbf{q} = q_r \hat{\mathbf{r}}$, where $\hat{\mathbf{r}}$ is the corresponding versor that is perpendicular to the spherical surfaces at each point and its sense is outwards the aforementioned surface. Taking this assumption into account, Equation (S-7) can be rewritten as:

$$\frac{1}{r^2} \frac{\mathrm{d}}{\mathrm{d}r} \left[r^2 \, q_r(r) \right] = 0. \tag{S-8}$$

Similarly, Fourier law takes the form:

$$q_r = -k \frac{\mathrm{d}T}{\mathrm{d}r}. \tag{S-9}$$

Then, by inserting Equation (S-9) into Equation (S-8) and simplifying we obtain:

$$\frac{\mathrm{d}}{\mathrm{d}r} \left[r^2 \frac{\mathrm{d}T(r)}{\mathrm{d}r} \right] = 0. \tag{S-10}$$

The solution of Equation (S-10) considering the boundary conditions $T(R_{\mathrm{in}}) = T_{\mathrm{in}}$ and $T(R_{\mathrm{out}}) = T_{\mathrm{out}}$ is (Carslaw & Jaeger, 1959):

$$T(r) = \frac{R_{\mathrm{out}} \, T_{\mathrm{out}} \left(r - R_{\mathrm{in}} \right) + R_{\mathrm{in}} T_{\mathrm{in}} \left(R_{\mathrm{out}} - r \right)}{\left(R_{\mathrm{out}} - R_{\mathrm{in}} \right) r}. \tag{S-11}$$

By virtue of Equation (S-9) we have:

$$q(r) = k \frac{\left(T_{\mathrm{in}} - T_{\mathrm{out}} \right)}{\left(R_{\mathrm{out}} - R_{\mathrm{in}} \right)} \frac{R_{\mathrm{out}} \, R_{\mathrm{in}}}{r^2}. \tag{S-12}$$

Thus, the heat flux through the inner spherical surface, crossing it radially outwards, is:

$$q(R_{\mathrm{in}}) = k \frac{\left(T_{\mathrm{in}} - T_{\mathrm{out}} \right)}{d} \frac{1}{1 - \tilde{\alpha}}, \tag{S-13}$$

where we have expressed R_{in} as $R_{\text{out}} - d$, where d is the thickness of the hollow sphere
(Figure S1), and defined $z = d/R_{\text{out}}$. Analogously, the heat flux through the outer sphere
is:

$$q(R_{\text{out}}) = k\frac{(T_{\text{in}} - T_{\text{out}})}{d}\left(1 - z\right). \tag{S-14}$$

In practice $z \ll 1$ and, consequently, Equation (S-13) can be rewritten as:

$$q(R_{\text{in}}) = k\frac{(T_{\text{in}} - T_{\text{out}})}{d}\left(1 + z + z^2 + \ldots\right), \tag{S-15}$$

It is very common in the specialized literature to consider only the zeroth order of approximation in both Equation (S-14) and Equation (S-15). In our work we will follow the same tendency, but we would like to pose the question to which extent the aforementioned approximation remains valid and to leave the discussion to a future work. In consequence, as long as the approximation $z \ll 1$ remains valid in Equations (S-14) and (S-15), the expression of the conductive heat flow corresponding to conductive heat transfer through a slab can be considered:

$$q^{\text{cond}} = k\frac{\Delta T}{d}. \tag{S-16}$$

Insertion of Equations (S-3) and (S-16) into Equation (S-4) leads to:

$$q^{\text{conv}} = k\left(\frac{2^4}{\text{Ra}_{\text{cr}}}\frac{\alpha\,\rho\,g\,\Delta T}{\kappa\,\eta}\right)^{\frac{1}{3}}\Delta T. \tag{S-17}$$

In the following, the superscript "conv" can be omitted. By comparing Equations (S-16) and (S-17) we can obtain an expression of the conductive lid thickness:

$$d = \left(\frac{\text{Ra}_{\text{cr}}\,\kappa\,\eta}{2^4\alpha\,\rho\,g\,\Delta T}\right)^{\frac{1}{3}}. \tag{S-18}$$

Thus, the right hand side of Equation (S-17) can be replaced by the right hand side of Equation (S-16) with d given by Equation (S-18).

May 27, 2021, 10:50am

If we assume that $T_1 > T_{\text{iso}} > T_2$ in Figure S2, then the incoming heat flux from below is given by Equation (S-17) in which $\Delta T = \Delta T_1 = T_1 - T_{\text{iso}}$, where T_{iso} is the isothermal temperature. The out-coming heat flux is also given by Equation (S-17) but $\Delta T = \Delta T_2 = T_{\text{iso}} - T_2$.

Thus, the expressions of the heat fluxes inside the Earth, which are the outgoing heat flux from the core and the heat fluxes incoming into and outgoing from the mantle, can be obtained in a straightforward fashion.

Text S2. Expression of the radioactive heat production rate

The expression of $H(t)$ was taken from the work by Turcotte and Schubert (2014), which we reproduce here.

$$
\begin{aligned}
H(t) = {}& 0.9928\, C_0^{\mathrm{U}} H_0 \left(^{238}\mathrm{U}\right) \exp\left[-\frac{\ln 2}{\tau_{\frac{1}{2}}\left(^{238}\mathrm{U}\right)}(t - t_0) \right] \\
& + 0.0071\, C_0^{\mathrm{U}} H_0 \left(^{235}\mathrm{U}\right) \exp\left[-\frac{\ln 2}{\tau_{\frac{1}{2}}\left(^{235}\mathrm{U}\right)}(t - t_0) \right] \\
& + C_0^{\mathrm{Th}} H_0 \left(^{232}\mathrm{Th}\right) \exp\left[-\frac{\ln 2}{\tau_{\frac{1}{2}}\left(^{232}\mathrm{Th}\right)}(t - t_0) \right] \\
& + 1.19 \times 10^{-4} C_0^{\mathrm{K}} H_0 \left(^{40}\mathrm{K}\right) \exp\left[-\frac{\ln 2}{\tau_{\frac{1}{2}}\left(^{40}\mathrm{K}\right)}(t - t_0) \right]. \quad \text{(S-19)}
\end{aligned}
$$

where C_0 and H_0 are the concentration and heat production rate per unit mass of each isotope at instant t_0, while $\tau_{\frac{1}{2}}$ is the corresponding half-life. In Table S1 we reproduce the values given in the work by Turcotte and Schubert (2014).

Text S3. Rheological models

The rheological response of a solid body is described by the complex Love numbers:

$$
K_{\mathrm{I}}(l, \omega_{lmpq}) = -\frac{3}{2} \frac{1}{l - 1} \frac{B_l \Im\left[\bar{J}(\chi)\right] \operatorname{sgn}\left(\omega_{lmpq}\right)}{\left(\Re\left[\bar{J}(\chi)\right] + B_l\right)^2 + \left(\Im\left[\bar{J}(\chi)\right]\right)^2}, \quad \text{(S-20)}
$$

in which $J(\chi)$ is defined by:

$$\bar{J}(\chi) = \int_0^\infty \dot{J}(t - t') \exp\left[-\mathrm{i}\chi(t - t')\right] \mathrm{d}t', \qquad (\text{S-21})$$

where the over-dot means differentiation with respect to t' and $\mathrm{i} = \sqrt{-1}$ is the imaginary unit. The particular form of the kernel $J(t - t')$ depends on the particular rheological model considered. However, it is generally given by:

$$J(t - t') = J(0)\,\Theta(t - t') + \text{viscous and hereditary terms}, \qquad (\text{S-22})$$

where $J(0)$ is the instantaneous value of the compliance which, in its turn, is the reciprocal value of the instantaneous rigidity $\mu(0)$, and $\Theta(t - t')$ is the Heaviside step function (Efroimsky, 2012).

The first term on the right hand side of Equation (S-22) describes the instantaneous elastic response in deformation of the body under stress. However, the general rheological response of a real solid body is a mixture of elastic and anelastic behavior. The latter includes viscous and hereditary behaviors.

The complex compliance is obtained from the *constitutive equation*, which relates stress and strain. In a linear medium, assumed to be homogeneous, incompressible and isotropic, the relationship between the components of the stress tensor and the strain tensor is, in general terms, given by:

$$2\,\bar{u}_{\gamma\nu}(\chi) = \bar{J}(\chi)\,\bar{\sigma}_{\gamma\nu}(\chi), \qquad (\text{S-23})$$

where $\bar{u}_{\gamma\nu}(\chi)$ and $\bar{\sigma}_{\gamma\nu}(\chi)$ are the complex counterparts of the strain and stress tensors, respectively (Efroimsky, 2012).

In our work, we will consider three rheological models to describe tidal dissipation within Earth's mantle, namely the Maxwell, the Burgers and Maxwell-Andrade models.

The Maxwell, Kelvin-Voigt and Burgers rheological models are typical examples of models used to describe different types of viscoelastic behavior of a solid body. The first one is represented as a dashpot and a spring connected in series. The second one is represented as a dashpot and a spring connected in parallel. These two models differ in at least two aspects. On one hand, after being deformed a body whose rheological behavior is characterized by the Maxwell model can not recover is shape. On the contrary, a body whose rheological behavior is described by the Kelvin-Voigt model, do recover its shape. On the other hand, in a Maxwell configuration, the applied stress acting on the spring and on the dashpot are equal, while the total deformation is the sum of the deformations of each of the aforementioned components.

The Burgers model can be thought as a Kelvin-Voigt element connected in series with a Maxwell element. It worth to note that the viscosity of the dashpot in the Kelvin-Voigt element has a different meaning from that of the viscosity of the dashpot in the Maxwell element (Renaud & Henning, 2018).

The last rheological model to be considered is that of Maxwell-Andrade. It is schematically similar to the Burgers model, but has the fundamental difference that the viscosity of the dashpot and the compliance (or rigidity) of the spring in the Kelvin-Voigt element are not fixed but are variable in order to allow for the hereditary reaction behavior (Efroimsky, 2012; Renaud & Henning, 2018). As a consequence of this, the Burgers element does not exactly recover its original form, i.e. there is a certain "hysteresis". The origin of the latter is due to dislocations and vacancy flow within the material that responds according to this rheology.

Concerning the expression of the complex creep function, $\bar{J}(\chi)$, which is given in general terms by Equation (S-21), in the following we will present its specific from for each rheology in a suitable form for its translation into a computer code.

For the Maxwell model, the expression of $J(t - t')$, which was given in its general form in Equation (S-22), is (Efroimsky, 2012):

$$J(t - t') = \left[J + (t - t') \frac{1}{\eta} \right] \Theta(t - t'). \qquad \text{(S-24)}$$

Inserting Equation (S-24) in Equation (S-21), and performing the required mathematical operations, we obtain:

$$\bar{J}(\chi) = J - \frac{i}{\chi \eta}. \qquad \text{(S-25)}$$

The real and imaginary parts of the right hand side of Equation (S-25) are evidently:

$$\Re \left[\bar{J}(\chi) \right] = J \qquad \text{(S-26a)}$$

$$\Im \left[\bar{J}(\chi) \right] = -\frac{1}{\chi \eta}. \qquad \text{(S-26b)}$$

The next step would be to insert Equations (S-26) into Equations (S-20). However, the presence of the tidal frequency in the denominator on the right hand side of Equation (S-26b) can cause numerical instabilities, given the possibility that χ can become zero when the considered rotating body crosses or gets captured in a spin-orbit resonance (Efroimsky, 2012). In order to avoid this numerical difficulty, we can define the dimensionless complex compliance $\mathcal{J}(\chi)$ as:

$$\mathcal{J}(\chi) = \eta \chi \bar{J}(\chi). \qquad \text{(S-27)}$$

By multiplying and dividing the right hand sides of Equations (S-20) by $\eta^2 \chi^2$, we can express the tidal quality functions in terms of the dimensionless complex compliance:

$$K_{\mathrm{I}}(l, \omega_{lmpq}) = -\frac{3}{2} \frac{1}{l-1} \frac{B_l \, \eta \, \chi \, \Im\left[\mathcal{J}(\chi)\right] \mathrm{sgn}\left(\omega_{lmpq}\right)}{\left(\Re\left[\mathcal{J}(\chi)\right] + B_l \, \eta \, \chi\right)^2 + \left(\Im\left[\mathcal{J}(\chi)\right]\right)^2}. \tag{S-28}$$

Using Equation (S-25) and Equation (S-27), the dimensionless creep response function for the Maxwell rheology is:

$$\mathcal{J}(\chi) = J \, \eta \, \chi - \mathrm{i}, \tag{S-29}$$

whose real and imaginary parts are:

$$\Re\left[\mathcal{J}(\chi)\right] = J \, \eta \, \chi \tag{S-30a}$$

$$\Im\left[\mathcal{J}(\chi)\right] = -1. \tag{S-30b}$$

Inserting Equations (S-30) into Equations (S-28) we obtain:

$$K_{\mathrm{I}}(l, \omega_{lmpq}) = \frac{3}{2} \frac{1}{l-1} \frac{B_l \, \eta \, \chi \, \mathrm{sgn}\left(\omega_{lmpq}\right)}{\left(J + B_l\right)^2 \eta^2 \, \chi^2 + 1}. \tag{S-31}$$

The rheology of a body described by the Maxwell model behaves as a elastic solid at high frequencies ($\chi \, \eta \, J \gg 1$). On the contrary, at low frequencies, it behaves as a viscous solid body ($\chi \, \eta \, J \ll 1$). Consequently, this kind of behavior has the particular feature of underestimate tidal dissipation at high frequencies. In order to overcome this inconvenience, more realistic rheologies can be considered such as the Burgers and Maxwell-Andrade models.

The complex compliance function corresponding to the Burgers model is given by (Renaud & Henning, 2018):

$$\bar{J}(\chi) = J - \frac{\mathrm{i}}{\eta \, \chi} + J_{\mathrm{R}} \left(\frac{1 - \mathrm{i} \, J_{\mathrm{R}} \, \eta_* \, \chi}{1 + \left(J_{\mathrm{R}} \, \eta_* \, \chi\right)^2}\right). \tag{S-32}$$

For the sake of reducing the number of free parameters, we follow the work by Renaud and Henning (2018), who expressed the relaxed compliance, J_{R}, and the Kelvin-Voigt viscosity, η_*, in terms of the unrelaxed compliance, J, and the Maxwell viscosity, η, as follows:

$$J_{\mathrm{R}} = \zeta_{\mathrm{J}}\, J, \tag{S-33a}$$

y

$$\eta_* = \zeta_\eta\, \eta. \tag{S-33b}$$

For the Earth's mantle, the parameters ζ_{J} and ζ_η are taken equal to 0.2 and 0.02, respectively (Renaud & Henning, 2018).

The corresponding expression of the dimensionless complex compliance is:

$$\mathcal{J}(\chi) = J\,\eta\,\chi - \mathrm{i} + \zeta_{\mathrm{J}}\, J\,\eta\,\chi \left(\frac{1 - \mathrm{i}\,\zeta_{\mathrm{J}}\,\zeta_\eta\, J\,\eta\,\chi}{1 + \left(\zeta_{\mathrm{J}}\,\zeta_\eta\, J\,\eta\,\chi\right)^2} \right), \tag{S-34}$$

while its real and imaginary parts are:

$$\Re\left[\mathcal{J}(\chi)\right] = J\,\eta\,\chi \left(1 + \frac{\zeta_{\mathrm{J}}}{1 + \left(\zeta_{\mathrm{J}}\,\zeta_\eta\, J\,\eta\,\chi\right)^2} \right) \tag{S-35a}$$

$$\Im\left[\mathcal{J}(\chi)\right] = -\left(1 + \frac{\zeta_\eta\left(\zeta_{\mathrm{J}}\, J\,\eta\,\chi\right)^2}{1 + \left(\zeta_{\mathrm{J}}\,\zeta_\eta\, J\,\eta\,\chi\right)^2} \right). \tag{S-35b}$$

These expressions combined with Equations (S-28) deliver the values of $K_{\mathrm{I}}\left(l, \omega_{lmpq}\right)$.

Similarly, the complex creep response function corresponding to the Maxwell-Andrade model is given by:

$$\bar{J}(\chi) = J - \frac{\mathrm{i}}{\eta\,\chi} + \frac{J^{1-\alpha}}{\left(\mathrm{i}\,\zeta_{\mathrm{A}}\,\eta\,\chi\right)}\Gamma\left(1 + \alpha\right), \tag{S-36}$$

where α is known as Andrade's parameter and ζ_{A} is identified with the ratio between the characteristic times of the Maxwell-Andrade rheology (τ_{A}) and that of the viscoelastic response (τ_{M}). In general, due to the current lack of knowledge about this particular

aspect, it is common to set $\zeta_A = 1$, which implies $\tau_A = \tau_M$. This last equality is approximately true for relatively low stresses, such as the ones we have in this kind of study (Castillo-Rogez et al., 2011). On the other hand, Karato and Spetzler (1990) point out that the anelastic dissipation mechanism is effective in the Earth's mantle up to the limit frequency $\chi_0 \simeq 1$ year^{-1}. At lower frequencies, this mechanism is less efficient resulting in viscoelastic behavior. That is, at low frequencies the mantle behaves like a Maxwell solid. Consequently, for frequencies higher than χ_0, the anelasticity is the dominant dissipation mechanism and, therefore, in such a frequency regime the aforementioned equality is satisfied (Efroimsky, 2012).

Concerning the Andrade parameter, α, it should be noted that the values it assumes (which is specific to each material) are always in the interval $[0.14, 0.4]$ for all minerals, including ice, which constitutes a surprising fact (Efroimsky, 2012). The lower values of the interval correspond to materials at high temperatures or semi-molten and the higher values correspond to colder rocks and ices.

The dimensionless complex compliance function for Maxwell-Andrade rheology is given by:

$$\mathcal{J}(\chi) = J\eta\chi - \mathrm{i} + \frac{J\eta\chi}{(\zeta_A J\eta\chi)^\alpha} \exp\left(-\mathrm{i}\frac{\pi}{2}\alpha\right) \Gamma(1+\alpha). \qquad \text{(S-37)}$$

Then, the real and imaginary parts of $\mathcal{J}(\chi)$ for the same rheology are given by:

$$\Re[\mathcal{J}(\chi)] = J\eta\chi + \frac{J\eta\chi}{(\zeta_A J\eta\chi)^\alpha}\Gamma(1+\alpha)\cos\left(\frac{\pi}{2}\alpha\right), \qquad \text{(S-38a)}$$

$$\Im[\mathcal{J}(\chi)] = -1 - \frac{J\eta\chi}{(\zeta_A J\eta\chi)^\alpha}\Gamma(1+\alpha)\sin\left(\frac{\pi}{2}\alpha\right). \qquad \text{(S-38b)}$$

In the case that the response of certain material that makes up a celestial body is modeled with this rheology, the expressions given in Equation (S-38) have to be combined with Equations (S-28) in order to evaluate the tidal quality function $K_I(l, \omega_{lmpq})$.

May 27, 2021, 10:50am

References

Carslaw, H. S., & Jaeger, J. C. (1959). *Conduction of heat in solids.* Oxford Science publications.

Castillo-Rogez, J. C., Efroimsky, M., & Lainey, V. (2011). The tidal history of iapetus: Spin dynamics in the light of a refined dissipation model. *Journal of Geophysical Research: Planets*, *116*(E9), n/a–n/a. Retrieved from `http://dx.doi.org/10.1029/2010JE003664` (E09008) doi: 10.1029/2010JE003664

Efroimsky, M. (2012, March). Bodily tides near spin-orbit resonances. *Celestial Mechanics and Dynamical Astronomy*, *112*, 283-330. doi: 10.1007/s10569-011-9397-4

Karato, S., & Spetzler, H. A. (1990, November). Defect microdynamics in minerals and solid state mechanisms of seismic wave attenuation and velocity dispersion in the mantle. *Reviews of Geophysics*, *28*, 399-421. doi: 10.1029/RG028i004p00399

Renaud, J. P., & Henning, W. G. (2018, apr). Increased tidal dissipation using advanced rheological models: Implications for io and tidally active exoplanets. *The Astrophysical Journal*, *857*(2), 98. Retrieved from `https://doi.org/10.3847/1538-4357/aab784` doi: 10.3847/1538-4357/aab784

Stacey, F. D., & Davis, P. M. (2008). *Physics of the earth* (Fourth ed.). Cambridge University Press.

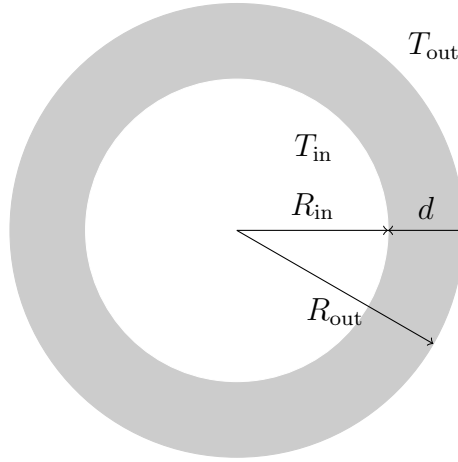Turcotte, D., & Schubert, G. (2014). *Geodynamics* (3rd ed.). Cambridge University Press.

Figure S1. Schematic representation of a hollow sphere with the representative parameters used to derive the thermal flux from the internal surface to the external surface through the volume enclosed by both surfaces.
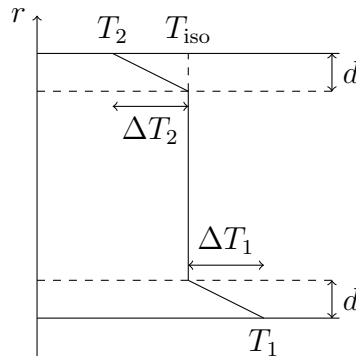

Figure S2. Vertical temperature profile in a setting where heat transport is dominated by convection.
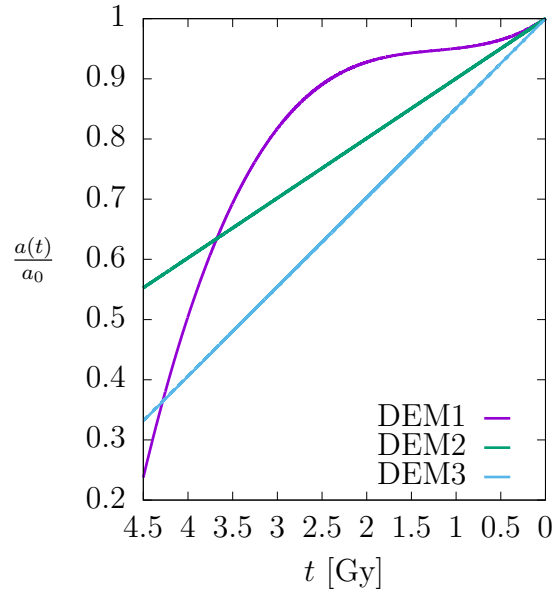
Figure S3. Plots of the three different assumed dynamical evolution models (DEMs) of the major semiaxis of the Moon's orbit
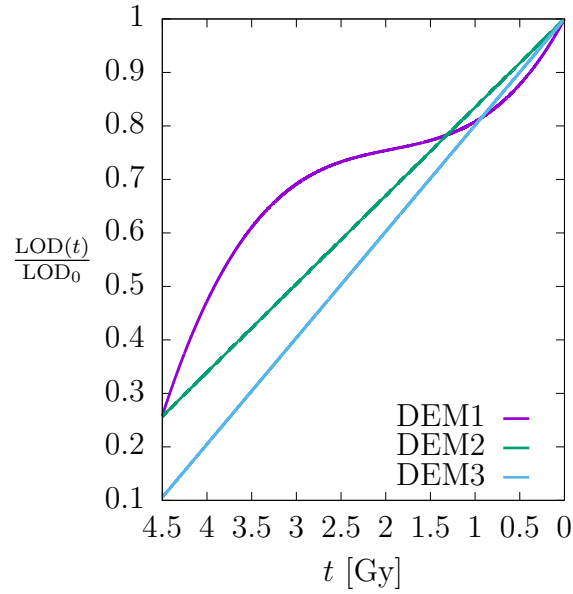

Figure S4. Plots of the three different assumed dynamical evolution models (DEMs) of the Earth's LOD.

May 27, 2021, 10:50am

Table S1. Thermally relevant radioactive isotopes together with the corresponding values of the parameters needed to compute the respective heat production rate per unit mass (Turcotte & Schubert, 2014).

Isotope	H_0 [W kg^{-1}]	$\tau_{\frac{1}{2}}$ [yr]	C_0 [kg kg^{-1}]
^{238}U	9.46×10^{-5}	4.47×10^{9}	30.8×10^{-9}
^{235}U	5.69×10^{-4}	7.04×10^{8}	0.22×10^{-9}
U	9.81×10^{-5}		31.0×10^{-9}
^{232}Th	2.64×10^{-5}	1.40×10^{10}	124×10^{-9}
^{40}K40	2.92×10^{-5}	1.25×10^{9}	36.9×10^{-9}
K	3.48×10^{-9}		31.0×10^{-5}

Table S2. Constants, physical and orbital parameters of the Earth-Moon system gathered from the works by (Stacey & Davis, 2008) and (Turcotte & Schubert, 2014).

Symbol	Value
G	6.67408×10^{-11}kg^{-1} m^3 s^{-2}
R_{gas}	8.31447 J K^{-1} mol^{-1}
$M_{\oplus}$	5.9722×10^{24}kg
$R_{\oplus}$	6.371×10^{6} m
R_{c}	3.480×10^{6} m
$M_{\C}$	7.342×10^{22} kg
ξ	$\frac{1}{3}$
μ	8.0×10^{10} Pa
η_{ref}	4.5×10^{21} Pa s
T_{ref}	1600.0 K
T_{s}	300.0 K
Ra_{cr}	1000
E^*	3.0×10^{5} J mol^{-1}
α	0.2
a	3.844×10^{8} m
e	0.0549
i	$\sim 23.5°$
P_{orb}	27.322 days

May 27, 2021, 10:50am

Table S3. Physical parameters and their corresponding numerical value for the core and mantle gathered from the works by (Stacey & Davis, 2008) and (Turcotte & Schubert, 2014).

Symbol	Unit	Core	Mantle
α	K^{-1}	1.0×10^{-5}	1.5×10^{-5}
ρ	$\mathrm{kg\,m}^{-3}$	1.076×10^{4}	4.5×10^{3}
g	$\mathrm{m\,s}^{-2}$	7.0	10.0
κ	$\mathrm{m}^2\mathrm{s}^{-1}$	6.0×10^{-6}	1.0×10^{-6}
k	$\mathrm{W\,K}^{-1}\mathrm{m}^{-1}$	36.0	6.0
ν	$\mathrm{m}^2\,\mathrm{s}^{-1}$	1.0	Variable